Low-Frequency Variability in the Equatorial Atlantic

R. H. WEISBERG AND A. M. HORIGAN[1]

Department of Marine Science and Engineering, North Carolina State University, Raleigh 27650

(Manuscript received 14 October 1980, in final form 4 April 1981)

ABSTRACT

Low-frequency v and u component oscillations in the eastern equatorial Atlantic are addressed using time series of up to 1.5 years duration from the lower portion of the main thermocline. A distinct frequency separation is observed with characteristic time scales of 1 month for v and 4–8 months for u. The principal v component oscillations correspond to seasonally modulated, linear, equatorially trapped Rossby-gravity waves, apparently generated at the surface in the central equatorial Atlantic by shear instability between the South Equatorial Current and the North Equatorial Countercurrent. Their length and time scales are well defined and they agree with theoretical predictions. The principal u component oscillations correspond to the deep zonal jets observed by recent profiling experiments in the Indian and Pacific Oceans. The vertical scales found here agree with the results from the other oceans; however, insufficient data are available anywhere to ascertain zonal scales. Linear theory would limit our observations to first meridional mode long or short Rossby waves or a Kelvin wave. Conjectures are made based upon ray tracing arguments, but unlike the linear v component oscillations, the u component scales suggest that they may intrinsically be nonlinear features. Theoretical guidance along with additional zonal- and vertical-length scale data are needed.

1. Introduction

The near-surface equatorial circulation consists of swift zonally oriented currents. The Equatorial Undercurrent is the most intense of these with speeds surpassing 100 cm s^{-1}. Recent measurements using free-falling velocity profiling systems have revealed the existence of equatorially confined zonal jets even at great depth. Luyten and Swallow (1976) first observed these in the Indian Ocean. Subsequently, they were found in the eastern and western portions of the Pacific Ocean by Hayes and Milburn (1980) and Eriksen (1981), respectively, and measurements from moorings to be presented here point to their presence in the Atlantic Ocean as well. These deep zonal jets appear to have vertical scales of several hundred meters, time scales of at least several months, and amplitudes ~ 20% of the near surface current values. Their study poses a formidable sampling problem. Small vertical scales require high vertical resolution as afforded by profilers while long (and as yet unknown) time scales require even longer serial observations as provided by moorings. In this paper we discuss low-frequency oscillations observed at several levels in the lower portion of the eastern equatorial Atlantic thermocline using time series of up to 1.5 years duration.

The data are outlined in Section 2. Section 3 contains a description of the low-frequency meridional (v) velocity component. In Section 4 the low-frequency zonal (u) velocity component is presented. The mean velocity component estimation is given in Section 5 and pertinent findings are discussed and summarized in Section 6.

2. Observations

The data were collected in the Gulf of Guinea (Fig. 1) at depths between 558 and 1936 m using subsurface moorings in a cooperative U.S.–French field program from June 1976–May 1978. Fig. 2 shows the velocity component data from the equator at 3°W, low-pass filtered to remove tidal and higher frequency oscillations. The complete data set is available in Weisberg *et al.* (1980) and Table 1 lists the locations and durations of the time series used herein.

Speeds typically range between ±15 cm s^{-1} with values as high as 30 cm s^{-1} which is similar to the profiling observations in other oceans. A distinct frequency separation is observed between the v and u components with v oscillating at a characteristic time scale of 1 month and u oscillating at 4–8 months. This is visually obvious in the E records and, excepting regions with topographic constraint, similar frequency separations between velocity components have not been observed elsewhere in the oceans. Kinetic energy distribution functions computed for v and u by ensemble averaging period-

[1] Deceased.

0022-3670/81/070913-08$06.00

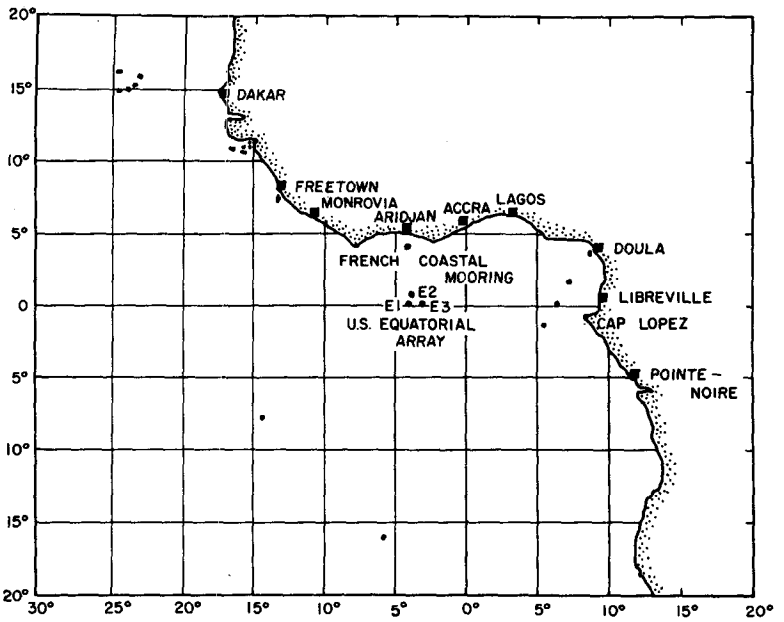

FIG. 1. Mooring locations in the Gulf of Guinea.

ograms over the three successive 6-month deployments, integrating over frequency, and normalizing by their respective variances quantify the separation as shown in Fig. 3. Roughly 59% of the u component variance occurs at time scales greater than two months compared to only 11% for the v component, while 51% of the v component variance occurs at time scales between three weeks and two months compared to only 15% for the u component. The half-power point separation between these v and u component processes is $\sim 8.3 \times 10^{-4}$ cph (cycles per hour). This affords independent resolution with 20 degrees of freedom so we will now examine these oscillations separately.

3. Low-frequency v component

Weisberg *et al.* (1979a) described the low-frequency v component oscillations as a narrow band packet of equatorially trapped Rossby-gravity waves. Analysis of the 6-month data subset spanning July 1977–January 1978 yielded a central periodicity of 31 days; upward and westward phase propagation with respective central wavelengths of 1000 m and 1200 km; downward and eastward energy flux with respective group velocity components of 0.014 and 16 cm s^{-1}; and equatorial confinement with an e-folding scale of 210 km.

Additional data now available corroborate and extend the previous analysis. We now have vertical length scale information over six pairs of time series during the E deployment with separations from 311 to 1264 m, rather than just one pair, and the time series length at the uppermost position is extended to 1.5 years.

Fig. 4 shows the vertical wavenumber component estimated from each of the six pairs as a function of depth. Upon scaling with the local buoyancy frequency, these estimates fall very close to a constant value in accordance with a WKB slowly varying medium approximation. The value of this constant, $\sqrt{gh}$, which is the separation parameter for the vertical and horizontal wave equations, agrees excellently with linear theory as calculated before.

To access the modulation of the low-frequency v component oscillations we decomposed the D31, E31 and F31 time series into 60-day overlapping segments and computed their spectra. Fig. 5 shows the v component variance at time scales longer than 12 days as a function of time along with the 90% confidence interval for random errors. Maximum energy occurs between the months of August and December. In comparing the confidence intervals at the peak month (October) with the minimum month (April), we see that they fail to overlap. The low-frequency v component appears to be nonstationary on the seasonal cycle.

The basis for the seasonal modulation of the Rossby-gravity waves probably resides with their generating mechanism. Legeckis (1977 and personal communication) observes seasonally modulated, 1-month periodicity, 1000 km wavelength meanders on the thermal front between the South Equatorial Current (SEC) and the North Equatorial Counter Current (NECC) in the Pacific and Atlantic Oceans in satellite imagery. Philander (1978) suggested a

meridional shear instability mechanism between these oppositely directed currents as a cause of the meanders. Cox (1980) then addressed the problem using a numerical model driven by seasonally varying winds and found a very closely tuned and seasonally modulated instability centered about the observed values. Fig. 6 from Katz (1977) shows the climatic mean wind-stress components averaged between 40 and 10°W in a band centered ±5° about the equator from the Atlantic Ocean. The wind stress goes through a seasonal cycle with maximum values from July through November and minimum values from February through April. The surface equatorial currents in the Atlantic Ocean as inferred from dynamic topography (Katz, 1981) parallel the seasonal cycle in the winds. Therefore, the observed Rossby-gravity wave modulation is consistent with generation by instability. A crude ray tracing using the calculated group velocity components and the local buoyancy frequency profile suggests that it had taken some 2–3 months for the wave packet to reach the observational depth and that it evolved in the central Atlantic around 15°W. If we scale the vertical wavelength observed at depth up to the surface in accordance with the buoyancy frequency we get an initial vertical scale of 100–200 m which matches the vertical scale of the currents.

4. Low-frequency *u* component

The principal *u* component time scale of 4–8 months, obtained from an ensemble average of all

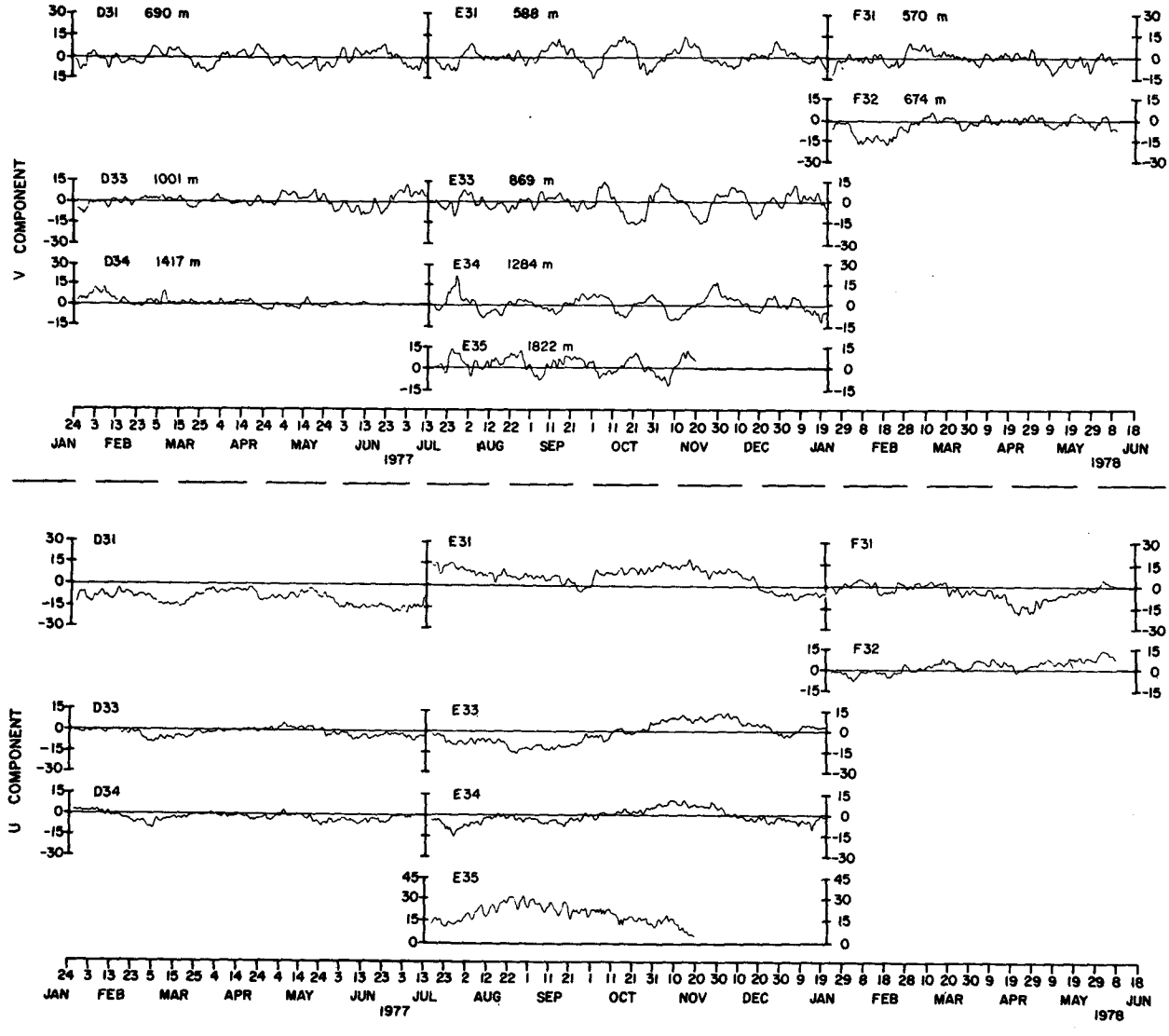

FIG. 2. Low-pass filtered *v* and *u* component time series from the D3, E3 and F3 deployments.

TABLE 1. Locations and durations of the time series used herein.

Data	Duration	Latitude	Longitude	Depth (m)
D11	1/31/77–7/8/77	0°02'S	4°02'W	568
D31	1/24/77–7/13/77	0°00'S	2°59'W	690
D32	1/24/77–6/25/77	"	"	794
D33	1/24/77–7/13/77	"	"	1001
D34	1/24/77–7/13/77	"	"	1417
E11	7/15/77–1/22/78	0°01'N	4°16'W	585
E1TC	"	"	"	586–626
E22	"	0°32'N	3°56'W	618
E31	"	0°03'S	3°09'W	558
E3TC	"	"	"	559–609
E33	"	"	"	869
E34	"	"	"	1284
E35	"	"	"	1822
F31	1/22/78–6/10/78	0°01'S	3°10'W	570
F32	"	"	"	674

periodograms, limited temporal sampling to only three realizations. However, the array provided excellent vertical resolution with separations ranging from 5 m (a thermistor chain) to 1264 m. Fig. 7 shows vertical wavenumber estimates as a function of depth computed for all instrument separations from cross-spectra averaged over time scales longer than 2 months (approximately six degrees of freedom). The symbols denote the realization and the numbers above each symbol give the vertical separation between instruments. With the exception of the 5–45 m separation point using a 50 m, 10-element, thermistor chain, all of the data points were computed from u components. The thermistor chain point was computed by linear least-squares fit to the phase as a function of separation for all possible combinations of thermistors. Confidence intervals are not shown since the limited degrees of freedom render the

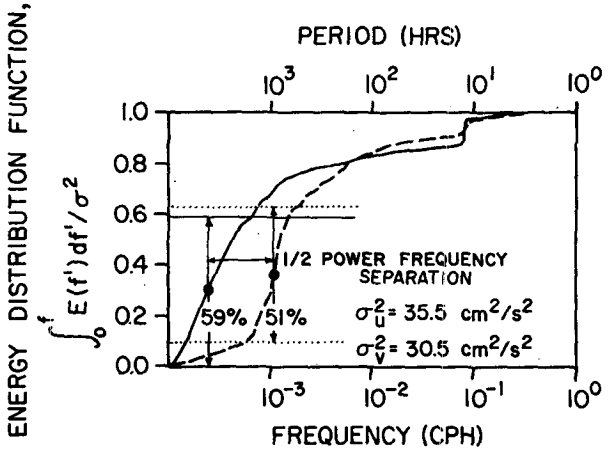

FIG. 3. Spectral energy distributions functions computed from the ensemble averaged periodigrams of records D31, E31 and F31 —a total of 1.5 years of data. $E(f)$ is the ensemble-averaged periodigram and σ^2 is the variance.

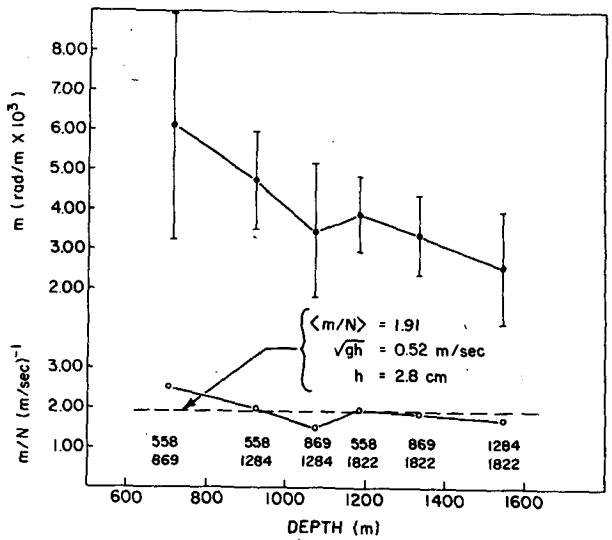

FIG. 4. The vertical wavenumber component estimates for the v component 1-month time-scale oscillations computed for each of the E3 instrument pairs. The open circles show the estimates after scaling by the local buoyancy frequency. 10% confidence intervals for random errors are shown for m.

phases statistically indeterminate; however, the net result covering three realizations in time suggest a mean vertical wavenumber directed upward with magnitude 0.0172 rad m^{-1} (365 m wavelength). Upon scaling with the buoyancy frequency, this corresponds to a separation parameter $\sqrt{gh}$ = 13.2 cm s^{-1}. From a plot of coherence as a function of separation using the 5–45 m and the 311 m thermistor separations (a thermistor chain and two VACM's) we estimated the vertical wavenumber bandwidth by linear least-squares fit to be ~0.002 rad m^{-1}. This agrees with the small scatter in Fig. 7 and demonstrates the rather narrow band nature of the low-frequency u component and temperature oscillations. The vertical wavelength estimate of 365 m plus or minus some 40–50 m (from the coherence determined bandwidth) also agrees qualitatively with the profiling measurements in other oceans cited in Section 1.

The low-frequency character of these zonal jets suggest either Rossby or Kelvin wave dynamics. For the former, the separation parameter $\sqrt{gh}$ determines a high-frequency cutoff. The non-dimensional dispersion relation for equatorial trapped waves on a β-plane (e.g., Moore and Philander, 1977) is

$$\omega^2 - k^2 - k\omega^{-1} = 2n + 1, \qquad (1)$$

where ω is the frequency, k is the zonal wavenumber component and n is the meridional mode number. For real valued k,

$$\omega^4 - 4(2n + 1)\omega^2 + 1 \geq 0. \qquad (2)$$

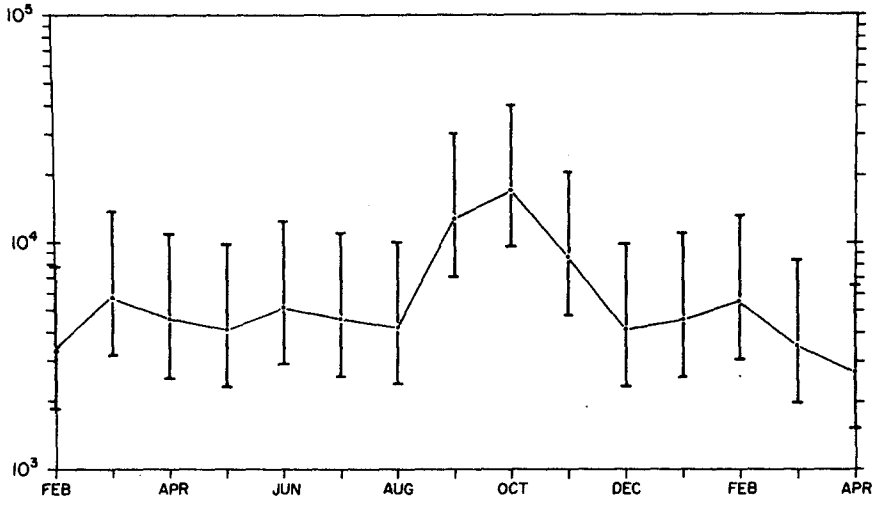

FIG. 5. Log$v$ component kinetic energy density as a function of time computed using 2-month overlapping segments, frequency averaged over time scales greater than 12 days. The bars denote the 90% confidence interval for random errors.

Rossby waves therefore have nondimensional frequencies less than

$$\{\tfrac{1}{2}(2n + 1) - [n(n + 1)]^{1/2}\}^{1/2},$$

while inertia-gravity waves have nondimensional frequencies greater than

$$\{\tfrac{1}{2}(2n + 1) + [n(n + 1)]^{1/2}\}^{1/2}.$$

The dimensional equivalents are $\omega(\beta\sqrt{gh})^{1/2}$ which, for $n = 1$, gives time scales greater than 4.8 months for Rossby waves and less than 24.5 days for inertia-gravity waves. Larger n leads to longer Rossby wave time scales and shorter inertia-gravity wave time scales. Thus, inertia-gravity wave dynamics are ruled out of the low-frequency observations. Furthermore, if one neglects the ω^4 term in Eq. (2) [dimensionally $\omega^2 \ll \beta\sqrt{gh}(2n + 1)$] then real valued k requires n to be less than or equal to $0.5[\beta\sqrt{gh}/4\omega^2 - 1]$ which limits the Rossby wave possibilities to $n = 1$ for the observed ω and $\sqrt{gh}$.

A very limited data subset was available for zonal wavenumber estimation. The D array provided a single current meter record and the E array provided both a current meter and a thermistor chain record at distances of 117 and 126 km west of their principal moorings, respectively. Cross spectra were averaged over time scales longer than two months and k was computed from all possible instrument pairs according to

$$k + m\cos\eta = \phi/D, \qquad (3)$$

where $\cos\eta$ is the directional cosine between the instrument pair displacement vector and the x axis, ϕ is the cross-spectral phase, and D is the separation between instruments. Owing to the array dimensions relative to the wave scales, multiples of 2π radians were subtracted from ϕ depending on the instrument pair used. The results are summarized in Fig. 8 (confidence intervals being excluded as in Fig. 7 for lack of sufficient degrees of freedom). Each point is a zonal wavenumber estimate, nondimensionalized using $\sqrt{gh} = 14$ cm s^{-1}, on an ordinate corresponding to a 200 day time scale chosen to best align the points with the nondimensional dispersion relations. Three possibilities exist: 1) Kelvin (closed circles), 2) long Rossby (open circles) and 3) short

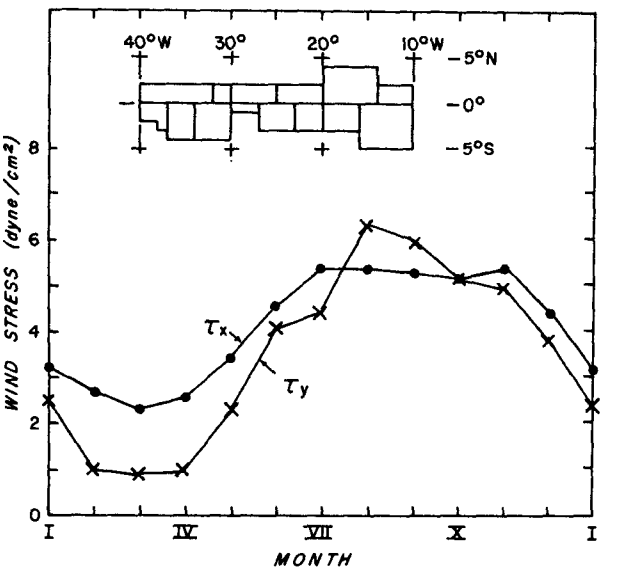

FIG. 6. Climatic monthly averaged wind stress components on the equator using data from the 14 subdivisions shown. The figure is from Katz (1977).

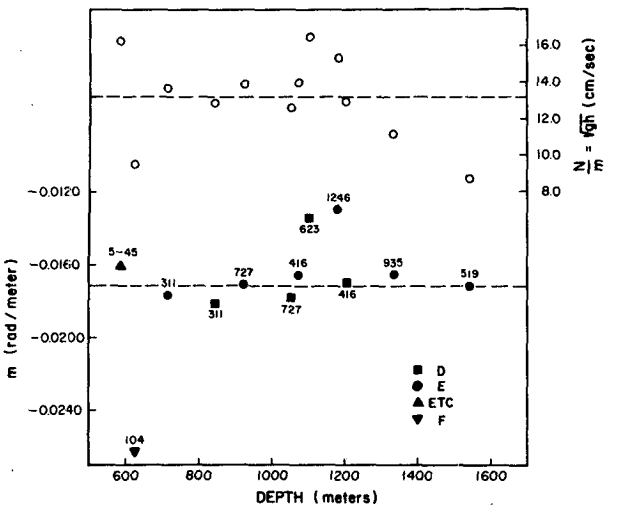

FIG. 7. Low-frequency u component vertical wavenumber estimates computed using all available record pairs. Cross spectra were averaged over time scales longer than 2 months. Open circles give separation parameter $\sqrt{gh}$ estimates by scaling with the local buoyancy frequency. Data from the D, E and F arrays are denoted in the legend.

Rossby (triangles) waves. The Kelvin and long Rossby wave points were obtained either directly or upon allowance for short vertical scale. The short Rossby wave points resulted from allowance for short zonal scale as well. Although they cluster about the dispersion curves, the data are inadequate to discriminate between the possibilities.

Neither the energy levels nor the phase relations between the velocity components and temperature offered further assistance. Lacking statistical significance but, nonetheless, properties of this particular data set, the energy levels did not scale vertically with the buoyancy frequency and the u to v component energy ratio of 7:1 for the single off-equator record did not agree with any of the linear wave eigenfunctions. Also, as noted by Eriksen (personal communication), the phase between the u component and temperature for vertically propagating waves should be $\pi/2$ but this was not observed.

5. Mean values

Fig. 2 shows that the v components at all sample depths (558–1936 m) oscillate about approximately zero mean values, while the u components oscillate about mean values with appreciable vertical shear. The principal v component time scale (1 month) being much shorter than the record length (1.5 years) allows for the assignment of a narrow confidence interval to the true mean value of v.

Under conditions, satisfied by the v component time series, that the autocovariance function $C(\xi)$ is absolutely integrable and that the lag time ξ for the autocovariance to approach zero is sufficiently shorter than the record length T, the variance of the mean value estimate $\hat{v}$ is given by (e.g., Papoulis, 1965):

$$\mathrm{var}\hat{v} = \frac{1}{T}\int_{\infty}^{\infty} C(\xi)d\xi, \tag{4}$$

which is equivalent to

$$\mathrm{var}\hat{v} = \frac{G(0)}{T}, \tag{5}$$

where $G(0)$ is the value of the autospectrum at zero frequency. Conceptually, $G(0)$ represents the portion of time series variance occurring at time scales

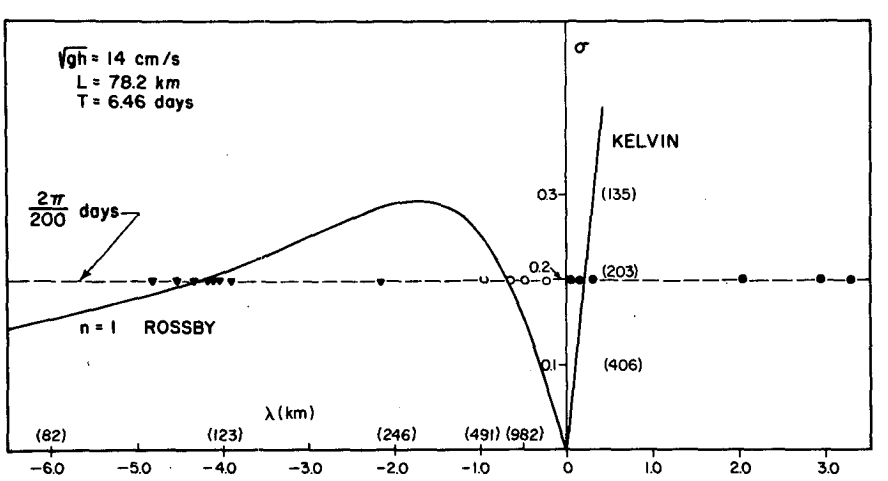

FIG. 8. Low-frequency u component zonal wavenumber estimates, nondimensionalized in accordance with the observed vertical scale and plotted relative to the dispersion curves for linear equatorially trapped Rossby and Kelvin waves. Dimensional scales are included in parentheses.

longer than the record length. It may be estimated by averaging over the lowest fundamental frequency bands for a desired number of degrees of freedom and confidence.

To estimate $G(0)$, we ensemble and frequency averaged the spectra from the three 6-month deployments at time scales greater than 2 months. Table 2 summarizes the variance of the mean estimation. It follows that the mean v component $\bar{v}$ is

$$\left.\begin{aligned}\bar{v} &= \hat{v} \pm (\mathrm{var}\hat{v})^{1/2} t_{n;0.1} \\ &= -0.2 \pm 0.8 \text{ cm s}^{-1}\end{aligned}\right\}, \tag{6}$$

with 90% confidence where $t_{n;0.1}$ is the 10 percentage point of the Student-t distribution.

We can conclude that the mean meridional velocity component over a major portion of the water column in the central Gulf of Guinea is not statistically different from zero with absolute value < 1 cm s^{-1}. This appears to be one of the few instances where the record length relative to the time scales of the data have allowed for such a restricted specification of an Eulerian mean. The observed absence of meridional transport across the equator in the central Gulf of Guinea confirms inferences drawn from the classical distribution of water properties as discussed for example by Defant (1961). Our observational depth range includes Antarctic Intermediate Water (AAIW) characterized by low salinity and high oxygen. A low-salinity tongue penetrates eastward along the equator accompanied by a negative oxygen gradient which has lead to the description of pure zonal advection along the equator at the depth range of the AAIW.

Further analysis of the Eulerian mean zonal circulation is deferred for two reasons. The vertical shear makes ensemble averaging inappropriate for data from different depths since the field is inhomogeneous and the data time scales are similar to the record lengths.

6. Discussion and summary

Separate low-frequency v and u velocity component oscillations were observed at depth on the equator in the eastern Atlantic Ocean. Their rectilinearity and alignment with the geographical coordinates are consistent with equatorial waveguiding.

The dominant v component time scale of approximately one month can be ascribed to seasonally modulated Rossby-gravity waves. These were initially discussed by Weisberg *et al.* (1979a). We have added additional data corroborating the previous results, and have demonstrated the seasonal modulation which suggests generation during the July–August maximum trade wind period in the central Atlantic. These Rossby-gravity waves appear to be a deep expression of waves generated by instability between the SEC and the NECC. As such they would provide a stabilizing effect for these major ocean currents by ridding them of excess energy. Indeed, during the GATE experiment, Weisberg *et al.* (1979b), Weisberg (1979) and Brown (1979) observed similar low-frequency features while at the same time unpublished *Trident* data (Miller *et al.*, 1976) showed a sudden (over less than one month) relaxation of the surface shear between the SEC and the NECC by a factor of 2.

The u-component oscillations appearing at much lower frequencies (4–8 months) had a well defined principal vertical length scale with upward phase propagation, but insufficient data were available to resolve either a zonal length scale or a propagation direction.

In terms of linear theory, the small vertical scale limits the choices to either long or short first meridional mode Rossby waves or a Kelvin wave. The zonal and vertical group velocity components available to these waves are, respectively,

$$\partial\sigma/\partial k = (2k + \beta/\sigma)/(2\sigma/gh + \beta/\sigma^2), \tag{7}$$

$$\partial\sigma/\partial m = \frac{[(2n+1)\beta - 2\sigma^2/(gh)^{1/2}]}{[N(2\sigma/gh + \beta k/\sigma^2)]} \tag{8}$$

for Rossby waves, and

$$\partial\sigma/\partial k = (gh)^{1/2}, \tag{9}$$

$$\partial\sigma/\partial m = \sigma(gh)^{1/2}/N \tag{10}$$

for Kelvin waves. Using the scales from Fig. 8, Table 3 gives component estimates, travel times to the observational depth, and zonal distances traversed over those times. Kelvin waves, if generated near the surface in the central or western Atlantic, travel fast enough to reflect off an eastern boundary as

TABLE 2. The variance of the mean v-component estimate.

$\langle G(0)\rangle$ (cm^2 s^{-2} cph^{-1})	ν	$t_{\nu,0.1}$	T (h)	var$\hat{v}$ (cm^2 s^{-2})
4578	20	1.325	11984	0.38

TABLE 3. Group velocity component estimates for long and short Rossby waves and for a Kelvin wave using values from Fig. 8, the associated travel times for energy to propagate 1000 m vertically with $N = 0.002$ s^{-1}, and the corresponding zonal distance covered during this time.

	$\frac{\partial\sigma}{\partial k}$ (cm s^{-1})	$\frac{\partial\sigma}{\partial m}$ (cm s^{-1})	ΔT (1000 m) (days)	ΔX (km)
Long	−3.0	-2.2×10^{-3}	526	1390
Short	+0.5	-3.6×10^{-4}	3215	1360
Kelvin	+14.0	-2.5×10^{-3}	463	5600

long Rossby waves before reaching the observational depth. Therefore, a predominance of linear Kelvin waves seems unlikely. Long and short Rossby waves have oppositely directed zonal group speeds. For a given vertical distance they traverse similar zonal distances with the long waves moving much faster. Short Rossby waves arriving at the observational site would be generated in the central portion of the Atlantic since their energy flux is eastward.

A potentially important finding is the relatively narrow vertical wavenumber bandwidth. Generation of narrow band waves by reflection is not expected, whereas generation by wave drag or instability might produce narrow band packets. Short Rossby waves are consistent with this type of generation since the eastward directed Equatorial Undercurrent is the principal momentum source on the equator.

Regardless of the above conjectures, a significant problem exists. The maximum zonal phase speeds for Kelvin and long Rossby waves are $(gh)^{1/2}$ and $\frac{1}{3}(gh)^{1/2}$, respectively. Short Rossby waves are slower. Given the small observed vertical scales, with $(gh)^{1/2}$ around 14 cm s^{-1}, relative to the observed u-component amplitudes in Fig. 2, it appears that the low-frequency u component oscillations, or deep zonal jets, are intrinsically nonlinear features (also pointed out by Eriksen, 1981). However, short vertical scales also could result from a linear superposition of wave modes. Here again the vertical wavenumber bandwidth obtained from coherence versus separation is an essential piece of information. Corroboration of the narrow band finding from longer time series or different ensemble members would argue against short vertical scales by random superposition of linear waves.

In summary, statistically and physically distinct low-frequency v and u-component behavior has been observed. The v component oscillations appear as linear, seasonally modulated expressions of nonlinearly generated waves. The u-component oscillations may be nonlinear. Their origin and dynamics remain as yet unknown. Theoretical guidance along with additional data on length scales (particularly zonal) and bandwidths (particularly vertical) are needed.

Acknowledgments. Support was provided by the Oceanography Section, National Science Foundation, under Grants OCE76-09786 and OCE78-20396. The Centre de Researches Oceanographiques, ORSTOM, Abidjan, Ivory Coast, assisted with the field work. J. Hickman assisted with the data management and computations and T. Clay assisted with the graphics.

REFERENCES

Brown, O. B., 1979: Observation of long period sea surface temperature variability during GATE. *Deep-Sea Res.*, **26**(Suppl. II), 103–124.

Cox, M. D., 1980: Generation and propagation of 30-day waves in a numerical model of the Pacific. *J. Phys. Oceanogr.*, **10**, 1168–1186.

Defant, A., 1961: *Physical Oceanography*, Vol. 1. Pergamon, 729 pp.

Eriksen, C. C., 1981: Deep currents and their interpretation as equatorial waves in the western Pacific Ocean. *J. Phys. Oceanogr.*, **11**, 48–70.

Hayes, S. P., and H. B. Milburn, 1980: On the vertical structure of velocity in the eastern equatorial Pacific. *J. Phys. Oceanogr.*, **10**, 633–635.

Katz, E. J., 1977: Zonal pressure gradient along the equatorial Atlantic. *J. Mar. Res.*, **35**, 293–307.

——, 1981: Dynamic topography of the sea surface in the equatorial Atlantic. *J. Mar. Res.*, **39**, 53–63.

Legeckis, R., 1977: Long waves in the eastern equatorial Pacific Ocean: A view from a geostationary satellite. *Science*, **197**, 1179–1181.

Luyten, J. R., and J. C. Swallow, 1976: Equatorial undercurrents. *Deep-Sea Res.*, **23**, 1005–1007.

Miller, L., R. H. Weisberg and J. A. Knauss, 1976: URI Hydrographic Observations During GATE: A report to the GATE equatorial and A-scale oceanographic workshop in Brest, France, 6–10 September 1976.

Moore, D. W., and S. G. H. Philander, 1977: Modelling of the tropical oceanic circulation. *The Sea*, Vol. 7, E. D. Goldberg. I. N. McCave, J. J. O'Brien and J. H. Steele, Eds., Wiley-Interscience, 319–361.

Papoulis, A., 1965: *Probability, Random Variables and Stochastic Processes*. McGraw-Hill, 583 pp.

Philander, S. G. H., 1978: Instabilities of equatorial currents, Part II. *J. Geophys. Res.*, **83**, 3679–3682.

Weisberg, R. H., 1979: Equatorial waves during GATE and their relation to the mean zonal circulation. *Deep-Sea Res.*, **26** (Suppl. II), 179–198.

——, A. M. Horigan and C. Colin, 1979a: Equatorially trapped Rossby-gravity wave propagation in the Gulf of Guinea. *J. Mar. Res.*, **37**, 67–86.

——, L. Miller, A. Horigan and J. A. Knauss, 1979b: Velocity observations in the equatorial thermocline during GATE. *Deep-Sea Res.*, **26**(Suppl. II), 217–248.

——, A. M. Horigan and J. H. Hickman, 1980: Equatorial subsurface velocity and temperature measurements in the Gulf of Guinea: July 1976–May 1978. Tech. Rep. 80-2, Dept. of Marine Science and Engineering, North Carolina State University, Raleigh.